Kinetics and Catalysis, Vol. 44, No. 2, 2003, pp. 165–174. Translated from Kinetika i Kataliz, Vol. 44, No. 2, 2003, pp. 179–189.

Intermetallic Hydrides $[TiFe_{0.95}Zr_{0.03}Mo_{0.02}]H_x$ ($0 \le x \le 2$): The Nature of the Phase Responsible for the Selective Reduction of CO_2[1]

D. I. Kochubei[1], V. V. Kriventsov[1], Yu. V. Maksimov[2], M. V. Tsodikov[3], F. A. Yandieva[3], V. P. Mordvin[4], J. A. Navio[5], and I. I. Moiseev[6]

[1] *Boreskov Institute of Catalysis, Siberian Division, Russian Academy of Sciences, Novosibirsk, 630090 Russia*

[2] *Semenov Institute of Chemical Physics, Russian Academy of Sciences, Moscow, 117912 Russia*

[3] *Topchiev Institute of Petrochemical Synthesis, Russian Academy of Sciences, Moscow, 117912 Russia*

[4] *Baikov Institute of Metallurgy, Russian Academy of Sciences, Moscow, 117911 Russia*

[5] *Institute of Materials Science, University of Seville, Seville, Spain*

[6] *Kurnakov Institute of General and Inorganic Chemistry, Russian Academy of Sciences, Moscow, 117912 Russia*

Received October 25, 2002

Abstract—Based on data obtained by X-ray diffraction and Mössbauer spectroscopy, it was concluded that tetragonal distortions appeared in the structure of cubic TiFe upon doping with Zr and Mo atoms and the intermetallide $TiFe_{0.95}Zr_{0.03}Mo_{0.02}$ is formed, which can absorb ~1 mol of H_2 per mole of the intermetallide. The heating of the hydrogen-saturated intermetallide in Ar to 185°C released ~0.80–0.82 mol of H_2 per mole of the intermetallide. This hydrogen was the constituent of cubic $[TiFe_{0.95}Zr_{0.03}Mo_{0.02}]H_{1.93}$ and orthorhombic $[TiFe_{0.95}Zr_{0.03}Mo_{0.02}]H$, which are the hydride phases of the parent $[TiFe_{0.95}Zr_{0.03}Mo_{0.02}]H_2$ hydride. The remainder of the hydrogen (~0.18 mol per mole of the intermetallide), which was released only at 700–920°C, entered the γ solution of nonstoichiometric TiH_{2-x}. EXAFS and XANES data indicate an increase in the signal intensity in the Ti–Ti direction and a decrease in electron density on titanium atoms for $[TiFe_{0.95}Zr_{0.03}Mo_{0.02}]H_{0.36}$. These results were interpreted in terms of a scheme according to which hydrogen atoms in an interstitial solid solution are arranged closer to titanium atoms and coordinated to them. It was found that a phase of $[TiFe_{0.95}Zr_{0.03}Mo_{0.02}]H_{0.36}$, which is a constituent of the γ solution, is responsible for the selective reduction of CO_2 to CO (90–98%).

INTRODUCTION

Hydrogen-accumulating metals and alloys attract interest as promising energy carriers, membranes, and catalyst components for various transformations of organic and inorganic compounds [1–6]. The catalytic activity of intermetallic systems based on nickel, zirconium, and rare-earth metals in hydrogenation and dehydrogenation reactions has been best studied [4–8].

The intermetallic hydride $[TiFe_{0.95}Zr_{0.03}Mo_{0.02}]H_x$ can reduce CO_2 at room temperature to result in the formation of CO and methane in small amounts [9]. It was found that 95–98% selectivity in CO formation could be reached in the reaction of CO_2 with this intermetallic compound at 350–430°C at a 60–70% conversion of carbon dioxide if a portion of hydrogen was preremoved from it. The α-TiFe alloy, which is a well-studied intermetallic compound, exhibits almost no catalytic activity in the hydrogenation of carbon dioxide [9–11].

These facts promted us to study the structure of $TiFe_{0.95}Zr_{0.03}Mo_{0.02}$ and its hydride phases in order to reveal factors responsible for the high activity and selectivity in the mild hydrogenation of CO_2.

EXPERIMENTAL

The intermetallide $TiFe_{0.95}Zr_{0.03}Mo_{0.02}$ and TiFe were prepared by the consumable-electrode arc melting of starting components. Titanium sponge (TG 100), low-carbon steel (GOST 11036-75), zirconium iodide, and molybdenum metal (MG1) were used as charge materials. To protect the alloy from the ingress of foreign impurities, the method of scull melting [12] was used in this study.

To evaluate absorption capacity, the isotherms of hydrogen absorption were obtained for the intermetallide and TiFe using a high-pressure manometric unit made of stainless steel. The alloys were crushed to a

[1] Paper presented at the 1st International Conference on Highly Organized Catalytic Systems (Chernogolovka, June 24–27, 2003).

0023-1584/03/4402-0165$25.00 © 2003 MAIK "Nauka / Interperiodica"

particle size of 0.5–1.0 mm; next, the particles were loaded into a reactor with a known volume. In each experiment, the weight of the alloy was 50 g. After loading, the reactor was evacuated to a pressure of 10^{-3} torr. Thereafter, the intermetallic compound in the reactor was activated by treatment with hydrogen at 70–80 atm and 20°C. The material was held under these conditions until the reactor began to heat; the heating was indicative of the chemical dissolution of hydrogen in the alloy. The time interval from the beginning of the treatment of the alloy with hydrogen to the beginning of reactor heating was designated as the activation period. After activating a sample, the reactor was completely pumped out and then filled with hydrogen to a certain pressure at 20°C. The amount of absorbed hydrogen was found from the difference between the initial and final pressures using the equation of state of a gas. The equilibrium pressures of hydrogen, which corresponded to each of the experimental points in an absorption curve, were obtained by maintaining the system for no less than 10 h after the establishment of a constant H_2 pressure, which was measured using a high-precision reference pressure gauge. We experimentally found that, in the course of H_2 absorption by the $TiFe_{0.95}Zr_{0.03}Mo_{0.02}$ intermetallide, ~1 mol of H_2 per mole of the intermetallic compound with the specified formula was absorbed. The activation period for an undoped TiFe alloy was longer than 24 h, which is much longer than the analogous period for the doped intermetallide (~0.5 h).

The temperature-programmed desorption of hydrogen from the $[TiFe_{0.95}Zr_{0.03}Mo_{0.02}]H_x$ hydride was performed on a flow-circulation unit with circulation in a flow of argon on heating to 920°C at a rate of 10 K/min. The desorbed hydrogen was determined by gas chromatography on an LKhM-80 instrument with a column (1.5 m × 4 mm) packed with an SKT carbon adsorbent at 60°C with the use of argon as the carrier gas and a TPI detector.

The following six samples were chosen for studying the structure and electronic properties of the test intermetallic compounds and their hydride forms: (1) an undoped TiFe intermetallide, which was chosen as a reference material; (2) the doped intermetallide $TiFe_{0.95}Zr_{0.03}Mo_{0.02}$ (IM); and intermetallic hydrides containing different amounts of absorbed H_2 with the empirical formulas (3) $[IM]H_2$, (4) [IM]H, and (5) $[IM]H_{0.36}$. A sample of $[IM]_f$ (6) was prepared by initially saturating [IM] with hydrogen and then subjecting the $[IM]H_2$ hydride species to thermal desorption (up to 350°C; Ar) and extracting residual H_2 from the sample by treatment with CO_2 under circulation conditions at 350°C for 4–6 h to almost complete termination of CO_2 conversion into CO as described elsewhere [9, 10].

Diffraction measurements were performed on a Dron 3M automated diffractometer with filtered CuK_α radiation. Phases were identified using the JCPDS-ICDD database. The average crystallite size was determined from the broadening of two Bragg reflections by the approximation method. Magnesium aluminum spinel calcined at 1400°C was used as a reference material (external standard) for the determination of the coherent-scattering region. The hydride forms of intermetallic compounds were studied in a gas-tight X-ray chamber closed with a polymer film; this allowed us to blow an inert gas or CO_2 through it.

Mössbauer spectra were measured on an electrodynamic instrument with a ^{57}Co source in a chromium matrix at 300 K. Isomer shifts were measured with reference to α-Fe. The spectra were treated by the least-squares technique for the 3/2 ⟶ 1/2 Mössbauer transition. The hydride forms of intermetallic compounds were studied in a special cuvette in a CO_2 atmosphere.

The Ti and Fe K-edge EXAFS spectra were measured on an EXAFS spectrometer at the Siberian Synchrotron Radiation Center using fluorescence detection at an electron energy of 2 GeV and an average current of 80 mA in the storage ring during measurements. A single Si(111) channel-cut monochromator crystal was used as a monochromator. The oscillating part of $\chi(k)$ was separated by the standard procedure [13]. The preedge region was extrapolated to the region of EXAFS oscillations using Victoreen polynomials [13]. A smooth portion of the absorption spectrum was separated using cubic splines. The inflection point at the absorption edge was taken as the starting point E_0 of the EXAFS spectrum. To obtain radial atomic distribution (RAD) functions, the $k^3\chi(k)$ Fourier transform was used in a wavenumber range of ~4.0–13.0 Å^{-1}. Structural information (interatomic distances, coordination numbers, and Debye factors) was obtained by the simulation of spectra subjected to Fourier filtration using the EXCURV 92 program [14] and invoking published X-ray diffraction data on bulk compounds to set the initial structural models. The Ti and Fe K-edge XANES spectra were measured under the same conditions but with a smaller energy step.

RESULTS AND DISCUSSION

Hydrogen Absorption

As can be seen in Fig. 1, the solubility of H_2 in $TiFe_{0.95}Zr_{0.03}Mo_{0.02}$ is much higher than that in TiFe at the same pressure of hydrogen. A plateau is clearly defined in the absorption isotherm of TiFe (Fig. 1); the saturation pressure $P(1) \simeq 12.5$ atm corresponds to the plateau. According to published data [15–17], the initial region of H_2 absorption by the TiFe intermetallide can be attributed to the formation of the α phase, a solid solution of hydrogen in the intermetallide with the composition $[TiFe]H_x$, where $x \approx 0.0$–0.1. The plateau is attributed to a mixture of α and β phases with transition to the single-phase state of the β solution. The region of the individual β phase corresponds to $x = 0.7$–0.8; thereafter, the isotherm exhibits an increase in the pres-

sure of hydrogen because of additional dissolution of hydrogen in the β phase. The isotherm of H_2 absorption by the $TiFe_{0.95}Zr_{0.03}Mo_{0.02}$ alloy also exhibits a plateau, which corresponds to a saturation pressure of ~2 atm (Fig. 1). After the plateau region, the absorption curve exhibits a dramatically increased branch.

Thus, the absorption data suggest that the interaction of H_2 with the $TiFe_{0.95}Zr_{0.03}Mo_{0.02}$ alloy is noticeably different from the interaction of H_2 with the undoped TiFe alloy: a hydride phase based on the intermetallic compound was formed at a considerably lower pressure (~2 atm) than that in the case of TiFe (12.5 atm). Moreover, the intermetallic compound is characterized by a much shorter activation period (~0.5 h) than TiFe (over 24 h).

It can be seen in Fig. 1 that, after attaining an H_2/[IM] molar ratio approximately equal to unity, the subsequent dissolution of hydrogen requires a dramatic increase in the pressure.

Thermal Desorption of Hydrogen from the Structure of [IM]H_2

The curve of the thermal desorption of absorbed hydrogen from a sample with the stoichiometric composition $[TiFe_{0.95}Zr_{0.03}Mo_{0.02}]H_2$ ($[IM]H_2$) in an argon atmosphere (Fig. 2) clearly exhibits three regions. The first of them corresponds to the intense release of ~0.80–0.82 mol of H_2 per mole of the sample on heating this hydride from 70 to 185°C. An insignificant amount of H_2 was released as the temperature was further increased. Starting at ~700 and up to 920°C, ~50% of the remainder of the hydrogen absorbed by the intermetallide was released (i.e., ~0.09 mol H_2 per mole of the intermetallic compound). Higher temperatures are required for the thermal desorption of the remainder of the hydrogen (~0.09 mol/mol). We tentatively designated the hydrogen released at section *1* of the thermal desorption curve (Fig. 2) as weakly bound hydrogen (WBH) with the structure of the intermetallic compound, whereas H_2 desorbed at high temperatures (700–920°C) was hereafter designated as strongly bound hydrogen (SBH).

Generally, the thermal removal of hydrogen from $(TiFe_{0.95}Zr_{0.03}Mo_{0.02})H_2$ in the range 70–920°C can be represented by the reaction scheme

$$\underset{[IM]H_2}{(TiFe_{0.95}Zr_{0.03}Mo_{0.02})H_2} \xrightarrow[WBH]{\text{Ar, 70–185°C}} \underset{[IM]H_{0.36}}{(TiFe_{0.95}Zr_{0.03}Mo_{0.02})H_{0.36}} \xrightarrow[1/2SBH]{\text{Ar, 700–920°C}} \underset{[IM]H_{0.18}}{(TiFe_{0.95}Zr_{0.03}Mo_{0.02})H_{0.18}}. \quad \text{(I)}$$

The $[TiFe_{0.95}Zr_{0.03}Mo_{0.02}]H_{0.36}$ material was stable over a range from 200 to 700°C, and it did not lose strongly bound hydrogen up to the upper limit of this range. Approximately half the strongly bound hydrogen was lost only as the temperature was further increased from 700 to 920°C, whereas the remainder of hydrogen cannot be thermally removed. Nevertheless, in the reaction with CO_2 at 350°C, hydrogen bound in the $[IM]H_{0.36}$ hydride was almost completely consumed in the selective conversion of carbon dioxide to carbon monoxide

$$[IM]H_{0.36} \xrightarrow[-CO,\ -H_2O,\ +CO_2]{\text{Ar, 700–920°C}} \begin{cases} [IM]H_{\sim 0.18} \\ [IM]_f, \end{cases} \quad \text{(II)}$$

where $f < 0.18$.

The reactivities of the $[IM]H_2$ and $[IM]H_{0.36}$ hydrides toward CO_2 are different. Thus, the selectivity of CO_2 reduction to CO reached 80% at a temperature of 350°C and a pressure of 50 atm in the presence of the fully saturated $[IM]H_2$ hydride; the hydrocarbon fraction of the gas mainly contained methane (16%), whereas in the presence of the partially saturated hydride containing strongly bound hydrogen the selectivity of CO formation reached 99% at a 50% conversion, and the methane content of the hydrocarbon fraction of the gas was no higher than 0.16% [9, 10].

The structures of the parent intermetallic compound and its hydride forms were studied using X-ray diffraction analysis, Mössbauer spectroscopy, EXAFS, and XANES.

Parent intermetallide IM. The main structural motif of parent IM (Fig. 3a) is characterized by reflections with the interplanar distances d = 0.2117, 0.1493, and 0.1220 nm, which were also observed in the cubic modification of the α-TiFe alloy [15, 16]. The difference between this sample and undoped α-TiFe consists in the fact that the X-ray diffraction pattern of IM at the angles $2\theta = 40.50°$ and 40.75° exhibits weak reflections with d = 0.222 and 0.216 nm. It is most likely that they can be explained by the presence of a tetragonally distorted structure due to the introduction of dopant elements, for which the lattice parameters are a = 2.976 Å and c = 3.032 Å.

The Mössbauer spectra of the undoped α-TiFe intermetallide and a Zr- and Mo-doped alloy, that is, $TiFe_{0.95}Zr_{0.03}Mo_{0.02}$, exhibit a single line with the isomer shift (IS), 0.16 ± 0.03 mm/s, and the line width Γ = 0.36 ± 0.03 mm/s (Figs. 4a, 4b). Parameters that correspond to the cubic structure of α-TiFe [17] will be used in the subsequent discussion as reference data in the analysis of doped alloy samples. The spectrum in Fig. 4b also contains a single line; however, the shape and total width of this line are different from the refer-

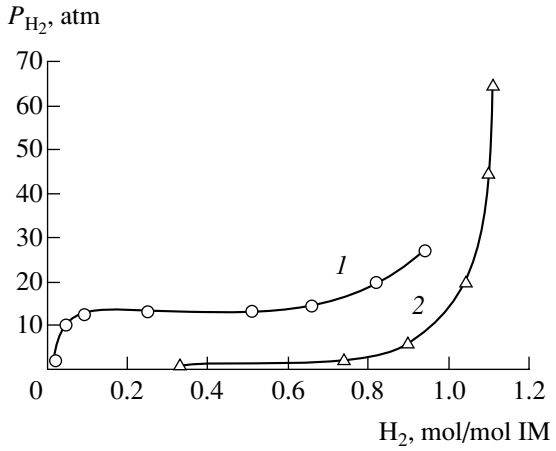

Fig. 1. Isotherms of hydrogen absorption in the (*1*) $TiFe–H_2$ and (*2*) $TiFe_{0.95}Zr_{0.03}Mo_{0.02}–H_2$ systems at 20°C.

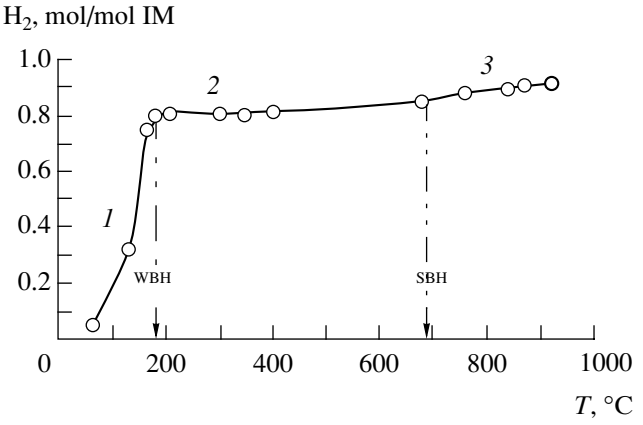

Fig. 2. Desorption of absorbed hydrogen from a sample of $[IM]H_2$ as the temperature was increased using linear programming.

ence values. A computer analysis allowed us to represent the spectrum as a superposition of a single line and a quadrupole doublet with the corresponding parameters IS = –0.17 ± 0.03 mm/s, Γ = 0.35 ± 0.03 mm/s, relative content δ = 0.74 and IS = –0.16 ± 0.03 mm/s, quadrupole splitting (QS) 0.35 ± 0.03 mm/s, Γ = 0.30 ± 0.03 mm/s, and δ = 0.26. As before, the single line corresponds to the cubic α-phase of the alloy, which was predominant in the IM sample. However, almost 1/3 of the $TiFe_{0.95}Zr_{0.03}Mo_{0.02}$ intermetallide structure includes spatial regions in which the local environment of Fe atoms is different from a spherically symmetrical (cubic) environment and is characterized by pronounced axial distortions, apparently because the atoms of the modifying elements are closely set.

This result is consistent with the X-ray diffraction (XRD) data; it suggests that the IM structure, which remained single-phase, was considerably distorted compared with the reference structure (α-TiFe). These distortions may be associated with shear deformations of the lattice because of the appearance of modifying additives in the form of zirconium and molybdenum atoms.

$[IM]H_2$ and [IM]H systems. After the absorption of the maximum amount of hydrogen by the $TiFe_{0.95}Zr_{0.03}Mo_{0.02}$ intermetallide (~1 mol of H_2 per 1 mol of IM), the phase composition of the intermetallide considerably changed. The sample became heterophasic with the predominance of a cubic modification isostructural to the γ-$TiFeH_{1.93}$ hydride [16] (*d* = 0.232, 0.2196, and 0.209 nm). An orthorhombic modification isostructural to β-TiFeH [16] (*d* = 0.2260, 0.2185, and 0.2156 nm) was present in a considerable, even if smaller, amount (Fig. 3b).

The Mössbauer spectrum of this sample (Fig. 4c) is also significantly different from the spectrum of the parent IM. The spectrum is described by two quadrupole doublets with the parameters IS = 0.07 ± 0.03 mm/s, QS = 0.29 ± 0.03 mm/s, Γ = 0.29 ± 0.03 mm/s, and δ = 0.39 and IS = 0.26 ± 0.03 mm/s, QS = 0.26 ± 0.03 mm/s, Γ = 0.30 ± 0.03 mm/s, and δ = 0.61, respectively. The former less intense doublet corresponds in its parameters to the orthorhombic structure of β-TiFeH, whereas the latter corresponds to the cubic γ-$TiFeH_{1.93}$ hydride [17].

Thus, the XRD data and Mössbauer spectra consistently indicate that the initial alloy structure in a sample of $[IM]H_2$ maximally saturated with hydrogen was completely rearranged, changing into a mixture of two modifications of intermetallic hydrides isostructural to the hydrides of TiFe [14–17].

The orthorhombic hydride modification isostructural to β-TiFeH [18] was predominant in the sample of [IM]H containing 0.5 mol of H_2 per 1 mol of IM, which was obtained after the removal of half the constituent hydrogen from $[IM]H_2$ (Fig. 3c). Weakly pronounced reflections from the cubic phase of the γ-$TiFeH_{1.93}$ type were also observed. Along with reflections due to these two hydrides, the X-ray diffraction pattern of [IM]H also exhibited reflections typical of the structure of $TiFeH_{0.06}$ [19] (*d* = 0.2106, 0.1485, and 0.1210 nm).

The Mössbauer spectrum of a sample of [IM]H (Fig. 4d) is described by three components: the most intense doublet with the parameters IS = –0.05 ± 0.03 mm/s, QS = 0.30 ± 0.03 mm/s, Γ = 0.33 ± 0.03 mm/s, and δ = 0.63 is close in parameters to the structure of β-TiFeH; a single line with the parameters IS = –0.10 ± 0.03 mm/s, Γ = 0.30 ± 0.03 mm/s, and δ = 0.34 belongs to α-$TiFe_{0.95}Zr_{0.03}Mo_{0.02}$; and a low-intensity doublet with the parameters IS = 0.30 ± 0.03 mm/s, QS = 0.27 ± 0.03 mm/s, Γ = 0.35 ± 0.03 mm/s, and δ = 0.03 is similar to the observed spectrum of the γ-$TiFeH_{1.93}$ hydride.

$[IM]H_{0.36}$ hydride. The $[IM]H_{0.36}$ hydride contains only strongly bound hydrogen. The X-ray diffraction pattern of this compound, which contains ~0.36 mol of hydrogen per 1 mol of IM (Fig. 3d) consists of a set of

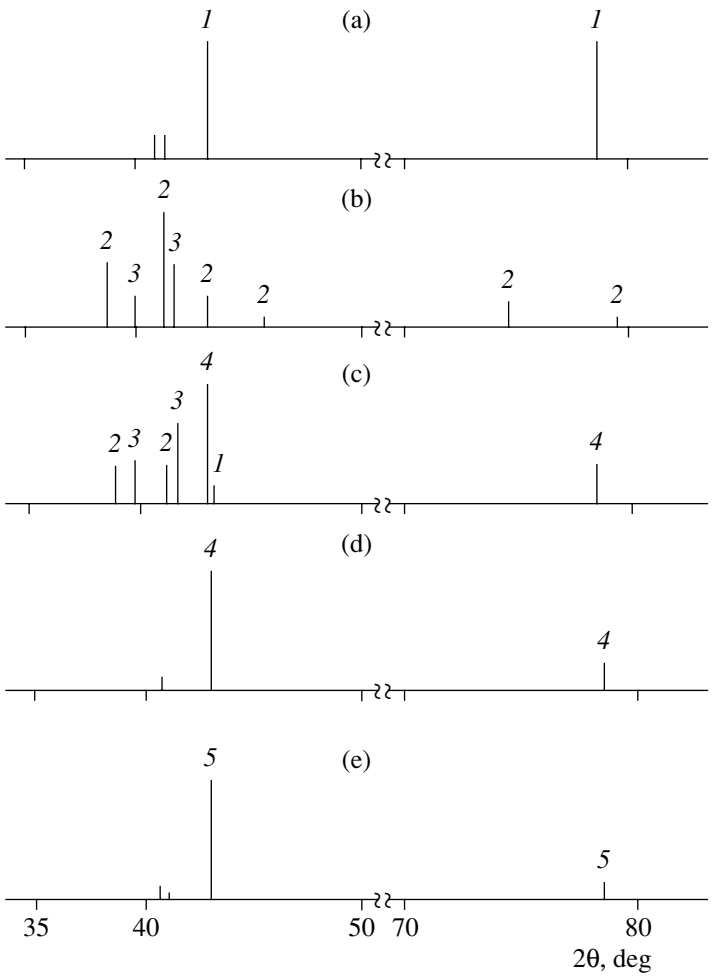

Fig. 3. Bar diagrams (XRD) for the initial $TiFe_{0.95}Zr_{0.03}Mo_{0.02}$ intermetallide and its hydride forms: (a) initial IM (without H_2 absorption); (b) $[IM]H_{1.93}$, absorbed 1 mol H_2/(mol IM); (c) [IM]H, absorbed 0.5 mol H_2/(mol IM); (d) $[IM]H_{0.36}$, after the thermal desorption of H_2 up to 350°C; (e) $[IM]H_f$, $0.36 \geqslant f \geq 0$, after reaction with CO_2. Line numbers correspond to the following phases: (*1, 2, 4, 5*) cubic phase and (*3*) orthorhombic phase.

lines with interplanar distances mainly related to a cubic modification isostructural to α-TiFe (Fig. 3d). In this case, it is likely that the reflection with d = 0.224 nm is also indicative of tetragonally distorted structures.

An analysis of [200] reflection profiles from the parent $TiFe_{0.95}Zr_{0.03}Mo_{0.02}$ intermetallide and the hydrogenated $[TiFe_{0.95}Zr_{0.03}Mo_{0.02}]H_{0.36}$ compound demonstrated that, after the removal of ~0.82 mol weakly bound hydrogen from the $[TiFe_{0.95}Zr_{0.03}Mo_{0.02}]H_2$ hydride, not only a shift of lines by $\sim\Delta 2\Theta = 0.02°$ but also a considerable line broadening compared with the initial intermetallide sample are observed. These changes are irreversible and also characteristic of $[IM]H_f$ (where $0.36 \geqslant f \geq 0$), which is obtained from $[IM]H_{0.36}$ after the almost complete removal of hydrogen as a result of treatment with CO_2 at 350°C (see scheme (III)).

The Mössbauer spectrum of the $[IM]H_{0.36}$ hydride is very similar to the spectrum of the parent IM alloy (Fig. 4b). Thus, it is also described by an intense single line and a doublet with the parameters IS = –0.14 ± 0.03 mm/s, Γ = 0.36 ± 0.03 mm/s, and δ = 0.74 and IS = –0.14 ± 0.03 mm/s, QS = 0.27 ± 0.03 mm/s, Γ = 0.28 ± 0.03 mm/s, and δ = 0.26, respectively. As in IM, the single line also characterizes the cubic α-alloy, whereas the doublet characterizes the alloy spatial regions in which the local environment of Fe atoms is different from a spherically symmetrical environment.

$[IM]H_f$ ($0.36 \geqslant f \geq 0$) system. Based on hydrogen balance, Tsodikov *et al.* [9] found that the $[TiFe_{0.95}Zr_{0.03}Mo_{0.02}]H_{0.36}$ intermetallide, which initially contained only strongly bound hydrogen and then was subjected to a long-term treatment with carbon dioxide at 350°C and a pressure of 15 atm, almost completely consumed this hydrogen in the selective reduction of CO_2 to CO:

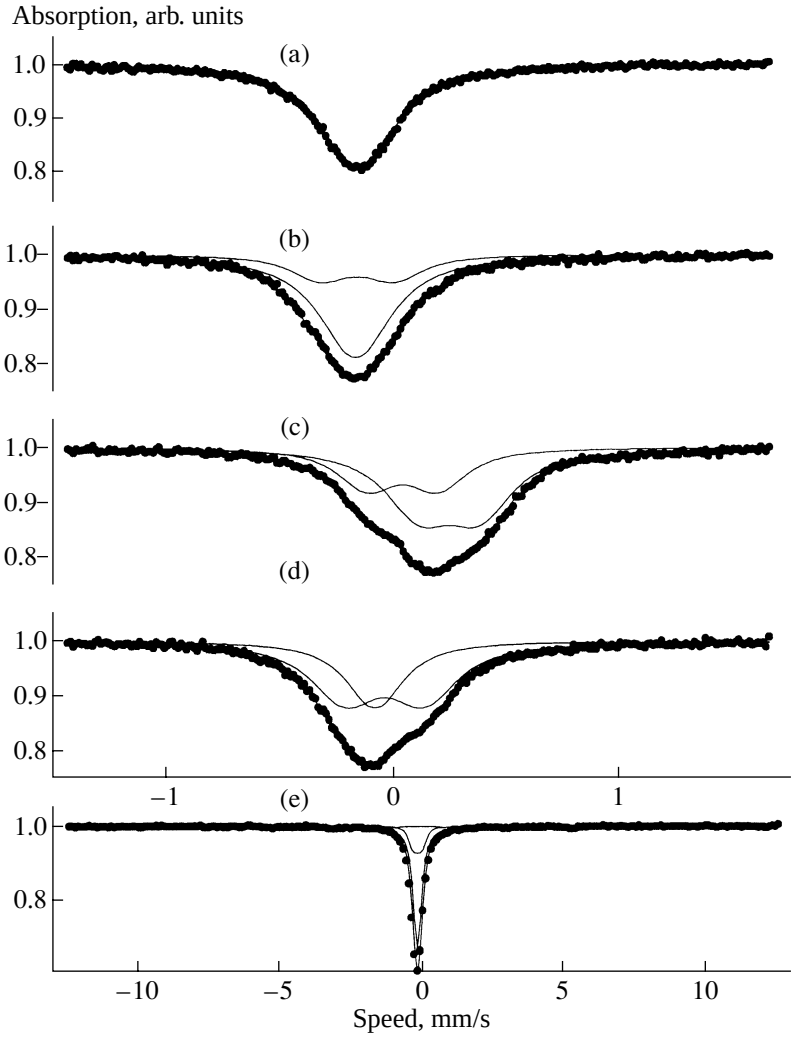

Fig. 4. Mössbauer spectra of α-TiFe, α-$TiFe_{0.95}Zr_{0.03}Mo_{0.02}$, and its hydride forms: (a) TiFe, (b) IM, (c) $[IM]H_2$, (d) [IM]H, and (e) $[IM]H_{0.36}$.

$$[TiFe_{0.95}Zr_{0.03}Mo_{0.02}]H_{0.36} \xrightarrow[+CO_2]{350^\circ C,\ 50\ atm} [TiFe_{0.95}Zr_{0.03}Mo_{0.02}]H_f + CO + H_2O, \quad \text{(III)}$$

where $0.36 \gg f \geq 0$

The X-ray diffraction pattern of a sample of $[IM]H_f$ exhibits, in addition to the most intense reflections that necessarily occur in a cubic modification of the α-TiFe alloy, reflections with d = 0.224 and 0.221 nm, which are indicative of a tetragonal distortion of the IM structure. It is typical that the relative intensity of these reflections increased compared with the sample of $[IM]H_{0.36}$ (cf. Figs. 3d, 3e). An analysis of these data suggests that the α-$TiFe_{0.95}Zr_{0.03}Mo_{0.02}$ phase both in samples containing strongly bound hydrogen (the $[IM]H_{0.36}$ compound) and in samples after the complete removal of strongly bound hydrogen (or at least the major portion of it, the $[IM]H_f$ compound) is not identical to the phase contained in the initial IM. The reflections of the samples of $[IM]H_f$ and $[IM]H_{0.36}$ were significantly broadened; this fact reflects a decrease in the average crystallite size of $[IM]H_f$ compared with the IM. The averaged size of parent IM crystallites corresponds to 85 nm, whereas the crystallite size of the sample of $[IM]H_f$ is 50 nm. Note that the intermetallide was decomposed as a result of the saturation of the parent IM with hydrogen and the removal of hydrogen from $[IM]H_2$ by thermal treatment and the subsequent elimination of hydrogen from $[IM]H_f$ in the reaction with CO_2.

In the Mössbauer spectrum of the sample of $[IM]H_f$, which was recorded over a wider range of source velocities with respect to the absorber (Fig. 4e), 95% reso-

nance absorption corresponded to "paramagnetic" phases of α-$TiFe_{0.95}Zr_{0.03}Mo_{0.02}$ (IS = –0.16 ± 0.03 mm/s, Γ = 0.34 ± 0.03 mm/s, and δ = 0.74) and to the doublet form of distorted areas of the structure of this phase (IS = –0.15 ± 0.03 mm/s, QS = 0.34 ± 0.03 mm/s, Γ = 0.28 ± 0.03 mm/s, and δ = 0.21).

The RAD curves of iron and titanium environments obtained from the corresponding EXAFS spectra (Figs. 5, 6) suggest that all the samples exhibit a well-resolved fine structure up to 8 Å. In this case, both hydrogen dissolution and almost complete hydrogen removal in reaction with carbon dioxide did not result in the appearance of new peaks.

It is well known that the structure of the TiFe intermetallide is a primitive cubic lattice in which each metal atom is surrounded with eight atoms of the other metal, which are located on cube corners with a distance of 2.56 Å, and with six atoms of the same metal, which constitute an octahedron with a distance of 2.98 Å [20] (Fig. 7). The environments of both of the chemical elements are identical. The distinctive feature of the IM alloy consists in the replacement of a portion of iron atoms with zirconium and molybdenum atoms. The simulation of EXAFS data for the initial IM is in good agreement with the known structure of α-TiFe. However, to obtain coordination numbers close to the observed values, very high Debye–Waller factors should be taken. This is due to the tetragonal distortion of the TiFe structure as it is changed into the test IM. A set of close interatomic distances appeared because of this structural distortion, and it is likely that the Debye approximation does not hold. In addition to iron atoms, Mo and Zr (which are absent from the model of TiFe used) also occur in the first coordination sphere of titanium. The RAD curves for the environments of titanium and iron are similar in the case of IM. The situation changed after the dissolution of hydrogen. Figure 6 demonstrates that the environment of iron remained unchanged both at a hydrogen content of 0.18 mol H_2 per mole of the sample and after the complete removal of hydrogen. A considerable change in the RAD curves of the environment of iron (a decrease in the intensity of reflections and the splitting of reflections) was observed only at high hydrogen contents: 1 and 0.5 mol H_2 per mole of the sample (the $[IM]H_{1.93}$ and [IM]H hydrides).

In contrast, the RAD curves that characterize the environment of titanium were dramatically changed on going from one hydride to the other (see Fig. 5). Thus, the presence of 0.18 mol H_2 in the $[IM]H_{0.36}$ intermetallide increased the intensity of peaks for the environment of titanium, as distinct from the RAD curves for iron. After the complete, or almost complete, removal of hydrogen from $[IM]H_f$, the RAD curves for both Ti and Fe became identical to that observed for the parent IM.

Two reasons for the changes in peak intensities in the RAD of titanium are plausible. First, it should be taken into account that the degree of structure distortion increased in the order TiFe ⟶ IM ⟶ $[IM]H_{0.36}$. However, this factor should result in analogous changes in the environment of not only titanium but also iron, which were not observed.

The second and most probable reason may be the unsymmetrical arrangement of the hydrogen atoms. According to neutron diffraction data, H atoms in the α- and δ-phases of the interstitial solid solutions of hydrogen in the TiFe intermetallide are localized at octahedral positions between four titanium atoms (with a Ti–H distance of 2.0 Å) and two iron atoms (with a Fe–H distance of 1.5 Å) (Fig. 7a) [18]. The Ti–H distance is typical of titanium hydride. Because iron does not form bulk hydrides, it is believed that hydrogen atoms are primarily bound to titanium, although the Ti–H interatomic distances are longer (as compared with Fe–H). However, the situation with the IM alloy is different because both zirconium and molybdenum can form hydrides. Therefore, a shift of hydrogen atoms from positions occupied in the TiFe alloy with a symmetrical octahedral arrangement of Ti and Fe atoms to dopant atoms of the intermetallide would be expected. The transition of hydrogen atoms to tetrahedral positions also cannot be excluded (Fig. 7b). In this case, these positions will be occupied first because they are more energetically favorable, whereas positions at iron atoms will be occupied secondarily at higher hydrogen concentrations. In particular, the anomalous behavior of $[IM]H_{0.36}$ hydride observed could be explained by the coordination of four H atoms around each impurity atom of Zr or Mo. In this case, the self-focusing effect of secondary photoelectrons, which is well known in EXAFS spectroscopy [13], would be expected. This effect is observed if a third atom falls on a straight line between the central and scattering atoms. The observed increase in peak intensity may be a manifestation of this effect.

All of the EXAFS data can be considered an indication that the atoms of strongly bound hydrogen in the $[IM]H_{0.36}$ hydride species are mainly bound to titanium atoms.

In terms of this scheme (i.e., the distribution of H atoms in $[IM]H_{0.36}$), the observed effect of the increase in RAD peak intensities for Ti in the $[IM]H_{0.36}$ hydride should be considered an indication that the H atom occurs in a position that is close to a straight line between the titanium and dopant atoms (Fig. 7b). This localization of H atoms may only be specific to the $TiFe_{0.95}Zr_{0.03}Mo_{0.02}$ intermetallide, and it forms the basis of not only the strong binding of hydrogen in hydrides but also the capability for selectively reacting with CO_2 at comparatively low temperatures. Note that such a binding was not observed in TiFe, and neutron diffraction data for the pure TiFe intermetallide with a high H_2 content [18] are indicative of a hydrogen atom localization thar differs from that in $[TiFe_{0.95}Zr_{0.03}Mo_{0.02}]H_{0.36}$.

An analysis of the XANES spectra allowed us to draw conclusions similar to those made from the

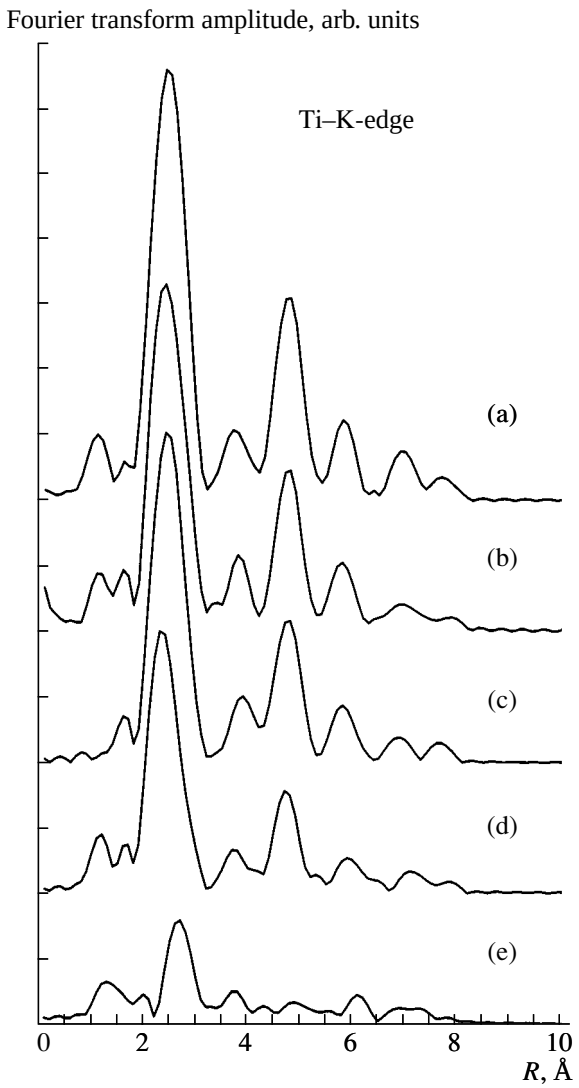

Fig. 5. RAD curves for the local environment of titanium: (a) IM, (b) $[IM]H_f$, (c) $[IM]H_{0.36}$, (d) [IM]H, and (e) $[IM]H_2$.

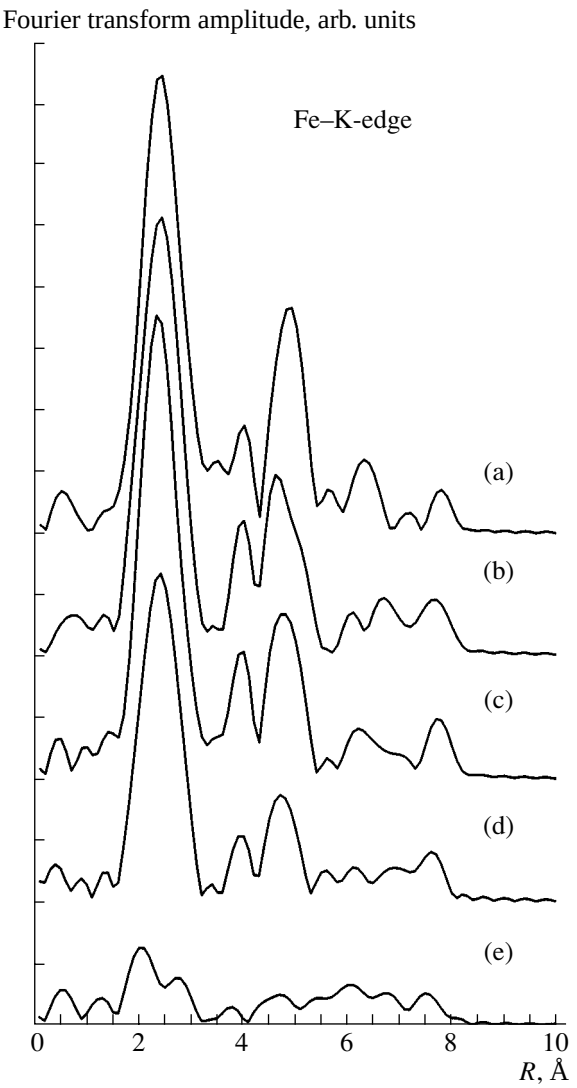

Fig. 6. RAD curves for the local environment of iron: (a) IM, (b) $[IM]H_f$, (c) $[IM]H_{0.36}$, (d) [IM]H, and (e) $[IM]H_2$.

EXAFS data. Changes in the XANES spectra for iron atoms (Fig. 8) were observed only at a hydrogen content higher than 0.18 mol H_2 per mole of the sample. Changes in the XANES spectra for titanium were observed at all of the concentrations of hydrogen (Fig. 9). However, the EXAFS data are indicative of reversible changes in the environment of titanium (i.e., the recovery of the intermetallide structure after the removal of hydrogen in a reaction with CO_2), whereas the state of atoms was irreversibly changed according to the XANES data. Thus, after hydrogen dissolution, the titanium absorption edge in the XANES spectrum of an intermetallide was shifted to higher energies, and this shift was retained after the removal of hydrogen by carbon dioxide. The shift of the absorption edge to higher energies can be interpreted as either a decrease in electron density at the metal atom due to electron-density transfer to the atoms of strongly bound hydrogen (primarily binding with titanium, hydrogen atoms in the test intermetallic compound are negatively charged, which is consistent with the data of quantum-chemical calculations for titanium hydride [21]) or a change in the distribution of the density of states of titanium *p*-electrons over the Fermi level due to a redistribution of electrons between levels. On detecting this effect, one should also taken into account that the saturation of an intermetallide with hydrogen results in its mechanical crushing. It is possible that this material degradation, which results in a transformation of granules into dust-like particles and which can be observed only visually, is based on deep structural changes. Thus, the dispersity of crystallites in the course of this process increased by almost 30%. The broadening of a coherent scattering spectrum, along with a noticeable increase in the specific surface area [9], is indicative of the formation of structural defects. The subsequent

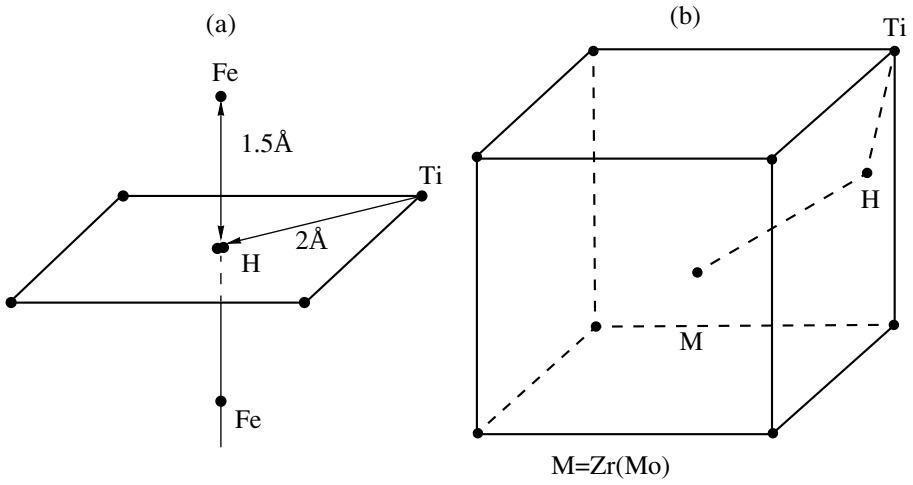

Fig. 7. Local structures of (a) the hydrogen-containing TiFeH polyhedron and (b) $[TiFe_{0.95}Zr_{0.03}Mo_{0.02}]H_{0.36}$.

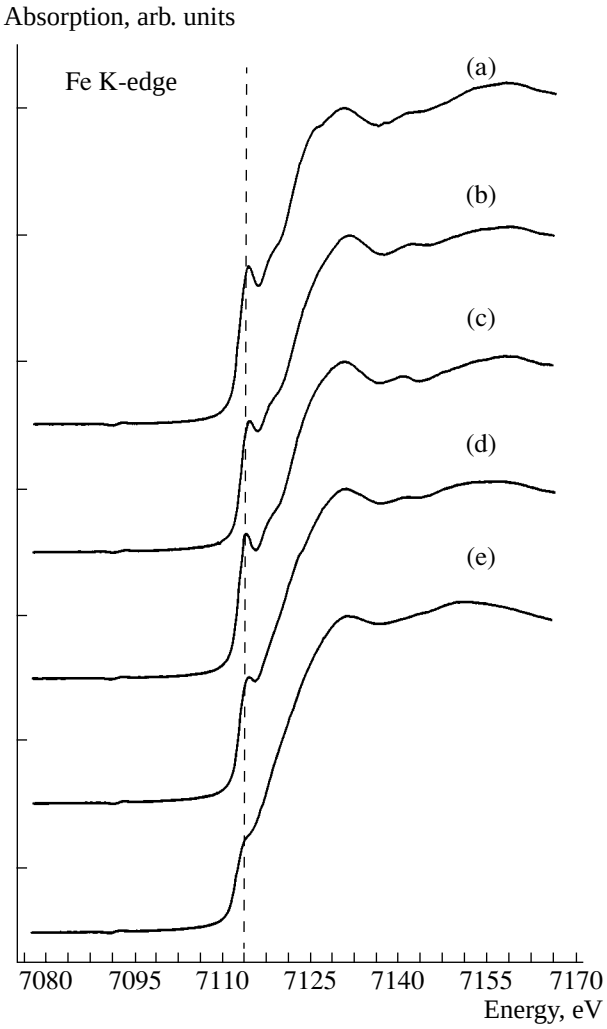

Fig. 8. XANES spectra (Fe K-edge): (a) IM, (b) $[IM]H_f$, (c) $[IM]H_{0.36}$, (d) [IM]H, and (e) $[IM]H_2$.

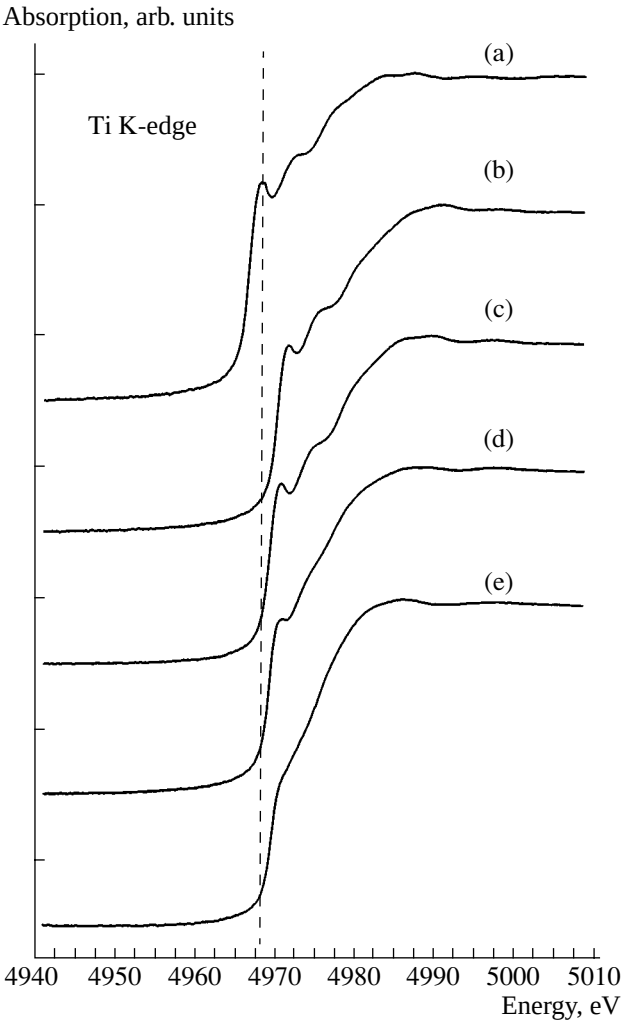

Fig. 9. XANES spectra (Ti K-edge): (a) IM, (b) $[IM]H_f$, (c) $[IM]H_{0.36}$, (d) [IM]H, and (e) $[IM]H_2$.

removal of hydrogen from the intermetallide structure probably favors an irreversible increase in the unsoundness due to the formation of vacancies at the titanium atoms, which bear a negative charge.

A special study is required to reveal the nature of processes responsible for the observed changes in the structure of intermetallic compounds.

CONCLUSIONS

The data obtained by X-ray diffraction and Mössbauer spectroscopy indicate that the introduction of Zr and Mo atoms in small amounts into an α-TiFe alloy with the formation of $[TiFe_{0.95}Zr_{0.03}Mo_{0.02}]$ resulted in a distortion of the highly symmetrical cubic structure of the parent binary intermetallide matrix. In this context, it is not surprising that the $TiFe_{0.95}Zr_{0.03}Mo_{0.02}$ alloy, which evidently has a set of unequal vacancies for the arrangement of atoms, absorbed 1 mol of H_2 per mole of titanium to form a set of metal hydrides. This mixture of hydride phases reduced carbon dioxide under very mild conditions, beginning at 20°C. However, the reaction is very nonselective; this is not surprising in the light of our data that are indicative of the existence of several phases in the hydride of $[TiFe_{0.95}Zr_{0.03}Mo_{0.02}]$.

After the thermal desorption of the most labile bound hydrogen species (weakly bound hydrogen), the temperature increased at which the reaction with carbon dioxide can occur. Evidently, residual hydrogen species after the removal of weakly bound hydrogen are less reactive toward CO_2 because these species are more strongly bound to the intermetallide lattice. At the same time, the reaction occurred more selectively and completed after the formation of CO. This suggests that the reaction pathway responsible for the conversion of CO_2 into methane and other hydrocarbons does not include the intermediate formation of CO. Note that the homologization of ethanol with carbon dioxide and hydrogen catalyzed by the Cu_3Zr_2Mn intermetallide [7, 8] also occurs without the intermediate formation of carbon monoxide.

The reactivity of strongly bound hydrogen in IM toward CO_2 hydrogenation and conceivable mechanisms of this reaction will be discussed elsewhere.

ACKNOWLEDGMENTS

This study was supported the NATO Research Center (project no. ENVIR.LG 971292).

REFERENCES

1. Buschow, K.J., Bouten, P.C.P., and Miedema, A.R., *Rep.Prog.Phys*, 1982, vol. 45, no. 9, p. 1039.
2. Lunin, V.V. and Kryukov, O.V., *Kataliz. Fundamental'nye i prikladnye issledovaniya* (Catalysis: Basic and Applied Studies), Petrich, O.A., Lunin, V.V., Eds., Moscow: Mos. Gos. Univ., 1987, p. 86.
3. Kalachev, B.A., Shalin, R.E., and Yalin, A.A., *Splavy – nakopiteli vodoroda* (Alloys for Hydrogen Storage), Moscow: Metallurgiya, 1995.
4. Chetina, O.V., Lunin, V.V., and Isagulyants, G.V., *Neftekhimiya*, 1988, vol. 28, no. 6, p. 757.
5. Lunin, V.V. and Chetina, O.V., *Zh. Fiz. Khim.*, 1990, vol. 64, no. 11, p. 3019.
6. Manovyan, K.A., Afanas'ev, P.V., and Lunin, V.V., *Kinet. Katal.*, 1992, vol. 33, no. 3, p. 566.
7. Evdokimova, E.V., Lunin, V.V., Afanasyev, P.V., and Moiseev, I.I., *Mendeleev Commun.*, 1993, no. 1, p. 1.
8. Moiseev, I.I., Evdokimova, E.V., Lunin, V.V., Afanas'ev, P.V., Gekhman, A.E., and Gromov, A.R., *Dokl. Ross. Akad. Nauk*, 1993, vol. 332, p. 195.
9. Tsodikov, M.V., Kugel', V.Ya., Slivinskii, E.V., and Mordovin, V.P., *Izv. Akad. Nauk, Ser. Khim.*, 1995, no. 10, p. 2066.
10. Tsodikov, M.V., Kugel, V.Ya., Yandieva, F.A., Slivinskii, E.V., Moiseev, I.I., Colon, G., Hidalgo, M.C., and Navio, J.A., *Stud. Surf. Sci. Catal.*, 2001, vol. 138, p. 239.
11. Tsodikov, M.V., Kugel', V.Ya., Yandieva, F.A., Slivinskii, E.V., Kochubei, D.I., Kriventsov, V.V., Gekhman, A.E., and Moiseev, I.I., Abstracts of Papers, *Rossiiskaya konferentsiya "Supramolekulyarnye soedineniya i aktivatsiya CO_2"* (Russian Conference on Supramolecular Compounds and CO_2 Activation), Cheboksary, 2001.
12. Mordovin, V.P., Tsodikov, M.V., Kugel', V.Ya., Vytnova, L.A., Slivinskii, E.V., and Yandieva, F.A., *Proc. II Int. Workshop on the Use of Energy-Accumulating Substances in Ecology, Machine Building, Energetics, Transport, and Space*, Moscow: Inst. Mashinoved., 2001, p. 121.
13. Kochubey, D.I., *EXAFS Spectroscopy of Catalysts*, Novosibirsk, Nauka, 1992.
14. Binsted, N., Campbell, J.V., Gurman, S.J., and Stephenson, P.C., *SERC Daresbury Laboratory EXCURV92 Program*, 1991.
15. *Hydrogen in Metals: Topics and Applied Physics. II Application – Oriented Properties*, Alefeld, G. and Volkl, J., Eds., Berlin: Springer, 1978, vol. 29.
16. Reilly, J.J. and Wiswall, R.H., *Inorg. Chem.*, 1974, vol. 13, p. 218.
17. Shenoy, G.K., Dunlab, B.D., Viccaro, P.J., and Niarehos, D., *Mössbauer Spectroscopy and Its Chemical Application*, Stevens, J.G. and Shenoy, G.K., Eds., 1981, p. 501.
18. Fischer, P., *Mater. Res. Bull.*, 1978, vol. 13, p. 931.
19. Thompson, P., *J. Phys., F*, 1980, vol. 10, p. 57.
20. Sakaki, S. and Ohkubo, K., *Inorg. Chem.*, 1989, vol. 28, p. 2583.
21. Ivanovsky, A.I., Gubanov, V.A., and Kurmaev, E.Z., *J. Phys. Chem.*, 1985, vol. 46, p. 823.